CHAPTER VI

CATALYTIC PROPERTIES OF Ni-Sn/$Ce_{0.75}Zr_{0.25}O_2$ CATALYSTS FOR METHANE PARTIAL OXIDATION

6.1 Abstract

In this study, Ni/$Ce_{0.75}Zr_{0.25}O_2$ catalyst was doped with different amounts of Sn by co-impregnation method. The catalysts were characterized by BET, H_2 chemisorption, XRD, TPR, TEM and tested for methane partial oxidation (MPO) to syngas in the temperature range of 400-800°C at atmospheric pressure. The results showed that Sn covered the surface of Ni particles and did not modify the bulk properties of the support. Addition of a small amount of Sn (< 0.5 wt%) lowered the catalytic activity for methane partial oxidation by less than 5% while the extent of carbon deposition was decreased by more than 50%. However, Sn loadings higher than 1 wt% caused a massive drop in catalytic activity. This indicates that as long as the Ni surface is only partially covered with Sn species, the active sites for the partial oxidation of methane remain intact, while the surface site ensembles required for carbon formation are blocked.

6.2 Introduction

Catalytic partial oxidation of methane to synthesis gas has been widely investigated for methane utilization as an alternative to the conventional steam reforming process. The process is exothermic and yields synthesis gas with a H_2/CO ratio of 2, which is suitable for methanol and Fisher-Tropsch synthesis. Many catalysts containing group VIII transition metals such as Ru, Rh, Pt, Pd and Ni (Dissanayake *et al.*, 1991; Hickman and Schmidt, 1993; Boucouvalas *et al.*, 1996; Otsuka *et al.*, 1998; Lu *et al.*, 1998, Pantu *et al.*, 2000) and metal oxides (Irigoyen *et al.*, 1998; Otsuka *et al.*, 1999; Ruckenstein and Hu, 1999) were employed for this reaction. Typical supported Ni catalysts are highly active for partial oxidation of methane to synthesis gas and inexpensive compared to noble metal catalysts (Montoya *et.al.*, 2000; Zhu and Stephanopoulos, 2001) but suffer from coke

deactivation. In a previous study (Pengpanich *et al.*, 2004), we reported that 5 wt%Ni/$Ce_{0.75}Zr_{0.25}O_2$ catalysts showed high activity, selectivity and stability for methane partial oxidation. Furthermore, this catalyst showed resistance to coke formation due to its high degree of metal dispersion and surface oxygen mobility. However, some carbon deposition was still observed.

Supported bimetallic catalysts are widely investigated. The addition of a second metal can improve the activity and/or selectivity of desired products and depress carbon deposition. Sn is well known as a promoter against carbon deposition in many processes such as aromatization and dehydrogenation of paraffins. Recently, the effects of Sn in the Ni-Sn supported catalysts have been investigated in steam, CO_2 reforming and partial oxidation of hydrocarbons (Ferreira *et al.*, 2003; Hou *et al.*, 2004; Nichio *et al.*, 2000). Hou *et al.* (2004) studied on Ni supported on α-Al_2O_3 reported that small amount of Sn loadings can be effectively used as promoter to reduce the amount of carbon deposition during CO_2 reforming of methane by improving the dispersion of Ni and retarding the sintering of active Ni particles during the reaction. This result is in agreement with Nichio *et al.* (2000). It was found that there is a range of tin concentrations (Sn/Ni atomic ratios < 0.05) for which the stability of the bimetallic catalysts is markedly enhanced with respect to nickel catalyst without affecting either the activity level or the selectivity to synthesis gas of methane partial oxidation and CO_2 reforming. The authors also concluded that the promoting effect of Sn atoms in intimate contact with nickel would be similar to what is proposed by Rostrup-Nielsen and Alstrup (1999) for the case of partly sulphur poisoned nickel catalysts.

In this study, Ni/$Ce_{0.75}Zr_{0.25}O_2$ catalyst was doped with different amounts of Sn and tested for methane partial oxidation to syngas in the temperature rage of 400-800°C at atmospheric pressure. The reducibility, characteristics and carbon deposition of Sn doped sample were also examined.

6.3 Experimental

6.3.1 Catalyst Preparation

Mixed oxide solid solution of $Ce_{0.75}Zr_{0.25}O_2$ supports was prepared via urea hydrolysis. The Ce-Zr mixed oxide sample was prepared from $Ce(NO_3)_3.6H_2O$ (99.0%, Fluka) and $ZrOCl_2.8H_2O$ (99.0%, Fluka). The synthesized procedure has been reported elsewhere (Pengpanich *et al.*, 2002).

The catalysts were prepared by co-impregnation method using the aqueous solutions of $Ni(NO_3)_2{\cdot}6H_2O$ and $SnCl_2{\cdot}2H_2O$ (99.0%, Fluka). The loading amount of Ni is 5 wt % and the amount of Sn loadings were varied between 0 and 2 wt% on supported Ni. The catalysts were then calcined at 500°C for 4 hr in air.

6.3.2 Catalyst Characterizations

BET surface area was determined by N_2 adsorption at 77 K (five point Brunauer-Emmett-Teller (BET) method using a Quantachrome Corporation Autosorb-1). Prior to the analysis, the samples were outgassed to eliminate volatile adsorbents on the surface at 250°C for 4 hr.

H_2 uptake and degree of dispersion were determined by using pulse technique (ThermoFinnigan modeled TPDRO 1100). About 250 mg of sample was place in quartz reactor. Prior to pulse chemisorption, the sample was reduce in H_2 atmosphere at 500°C for 1 hr. Then the sample was purged with N_2 at 500°C for 30 min and cooled to 50°C in flowing N_2. A H_2 pulse (pure H_2, 0.4 ml) was injected into the sample at 50°C. The metal dispersion was calculated by assuming the adsorption stoichiometry of one hydrogen atom per nickel surface atom.

A Rigagu X-ray diffractometer system equipped with a RINT 2000 wide-angle goniometer using CuK_α radiation and a power of 40 kV x 30 mA was used for examination of the crystalline structure. The intensity data were collected at 25 °C over a 2θ range of 20-90° with a scan speed of 5° (2θ)/min and a scan step of 0.02° (2θ).

The morphology of catalysts was observed by transmission electron microscopy (TEM) with a JEOL (JEM-2010F) transmission electron microscope

operated at 200 kV. The samples were dispersed in absolute ethanol ultrasonically, and the solutions were then dropped on copper grids coated with a lacey carbon film.

H_2-Temperature programmed reduction (TPR) measurements were carried out to investigate the redox properties over the resultant materials. In this study, H_2 was used as a reducing gas. H_2-TPR was carried out in TPR analyzer (Quantachrome modeled ChemBET- 3000 TPR/TPD). For this study, a 50 mg of sample was used. The sample was pretreated in flowing 20 ml/min N_2 atmosphere at 250°C for 30 min prior to running the TPR experiment, and then cooled down to room temperature in N_2. A 5% H_2 in N_2 gas at a flow rate of 75 ml/min was used as a reducing gas. The sample temperature was raised at a constant rate of 10°C/min from room temperature to 950°C. The amount of H_2 consumption during the increasing temperature period was determined by using a TCD signal.

Temperature programmed oxidation was carried out in TPO micro-reactor coupled to a FID analyszer. The TPO was used to determine the amount of carbonaceous deposition on the used catalysts. After running the reaction at 750°C for 24 hr, the catalyst was cooled down to room temperature in He. Then, about 30 mg sample was heated in a 2%O_2 in He (40 ml/min) at a heating rate 10°C/min up to 900°C. The output gas was passed to a methanation reactor using 15 wt% Ni/Al_2O_3 as a catalyst prior to FID detector. After the system reached 900°C, 100 µl of CO_2 pulses were injected in order to calculate the amount of coke on the catalyst.

6.3.3 Catalytic Activity Tests

Catalytic activity tests for methane oxidation were carried out in a packed-bed quartz tube microreactor (i.d. 6 mm). Typically, 100 mg of catalyst sample was packed between the layers of quartz wool. The reactor was placed in an electric furnace equipped with K-type thermocouples. The catalyst bed temperature was monitored and controlled by Shinko temperature controllers. Feed gas mixtures containing 4%CH_4, 2%O_2 and balanced He were used. The total flow rate of feed gas into the reactor was kept at 100 ml/min using Brooks mass flow controllers. The reactions were carried out at GHSV 50,000 hr^{-1}. The product gases were chromatographically analyzed using a Shimadzu GC 8A fitted with a thermal conductivity detector. A CTR I (Alltech) packed column was used to separate all

products at 50 °C except H_2O which was evaluated from the oxygen mole balance. Carbon balances were confirmed with all experiments conducted. The conversion of CH_4 (X_{CH_4}), O_2 consumption (X_{O_2}) and selectivities (S) reported in this work were calculated from:

$$\%X_{CH_4} = \frac{CH_4^{in} - CH_4^{out}}{CH_4^{in}} \times 100 \quad (3.3)$$

$$\%X_{O_2} = \frac{O_2^{in} - O_2^{out}}{O_2^{in}} \times 100 \quad (3.4)$$

$$\%S_{CO} = \frac{CO^{out}}{CO^{out} + CO_2^{out}} \times 100 \quad (3.5)$$

$$\%S_{H_2} = \frac{H_2^{out}}{H_2^{out} + H_2O^{out}} \times 100 \quad (3.6)$$

6.4 Results and Discussion

6.4.1 BET surface area, metal dispersion

The BET surface areas and metallic Ni dispersion of the catalysts are shown in Table 6.1. The BET surface areas of the catalysts are in the range of 51 – 66 m^2/g. It was found that the surface areas were slightly decreased by increasing Sn loading. This might be due to the fact that the coverage of Sn on the catalyst might hinder the access of N_2 during BET analysis.

The metal dispersions were also decreased by increasing amount of Sn. No adsorption of H_2 on $Sn/Ce_{0.75}Zr_{0.25}O_2$ was detected. This result indicated that the exposed Ni atom to H_2 is depressed by Sn.

Table 6.1 Characteristics of the catalysts, BET surface area and degree of dispersion of the catalysts

Catalyst code	Ni (wt%)	Sn (wt%)	Sn/Ni (atomic ratio)	BET Surface Area (m^2/g)	Dispersion (%)
5Ni00Sn	5	0	0	66	6.40
5Ni01Sn	5	0.1	0.01	64	4.98
5Ni03Sn	5	0.3	0.03	63	3.43
5Ni05Sn	5	0.5	0.05	61	2.58
5Ni10Sn	5	1	0.10	58	1.79
5Ni20Sn	5	2	0.20	51	0.90

6.4.2 XRD

The XRD patterns of Ni-Sn over $Ce_{0.75}Zr_{0.25}O_2$ catalysts after calcined at 500°C are shown in Figure 6.1. Similar to the XRD patterns of 5Ni00Sn catalyst, those of Ni-Sn over $Ce_{0.75}Zr_{0.25}O_2$ catalysts exhibited major peaks at about 28°, 33°, 47° and 58° (2θ) indicated a cubic fluorite structure of CeO_2. The small peak of NiO phase was observed at about 43° (2θ). No formations of single-phase Ni_3Sn, Ni_3Sn_2 and Ni_3Sn_4 were found by XRD. However, Onda *et al.* (2001) found that small peaks of these single-phases could be observed over Ni-Sn/SiO_2 prepared by chemical vapor deposition technique with 5 wt% Ni and a Sn/Ni atomic ratio of 0.3. The absence of these peaks in our study may be owe to the fact that the low amount of metal loading could not be captured by the XRD analysis.

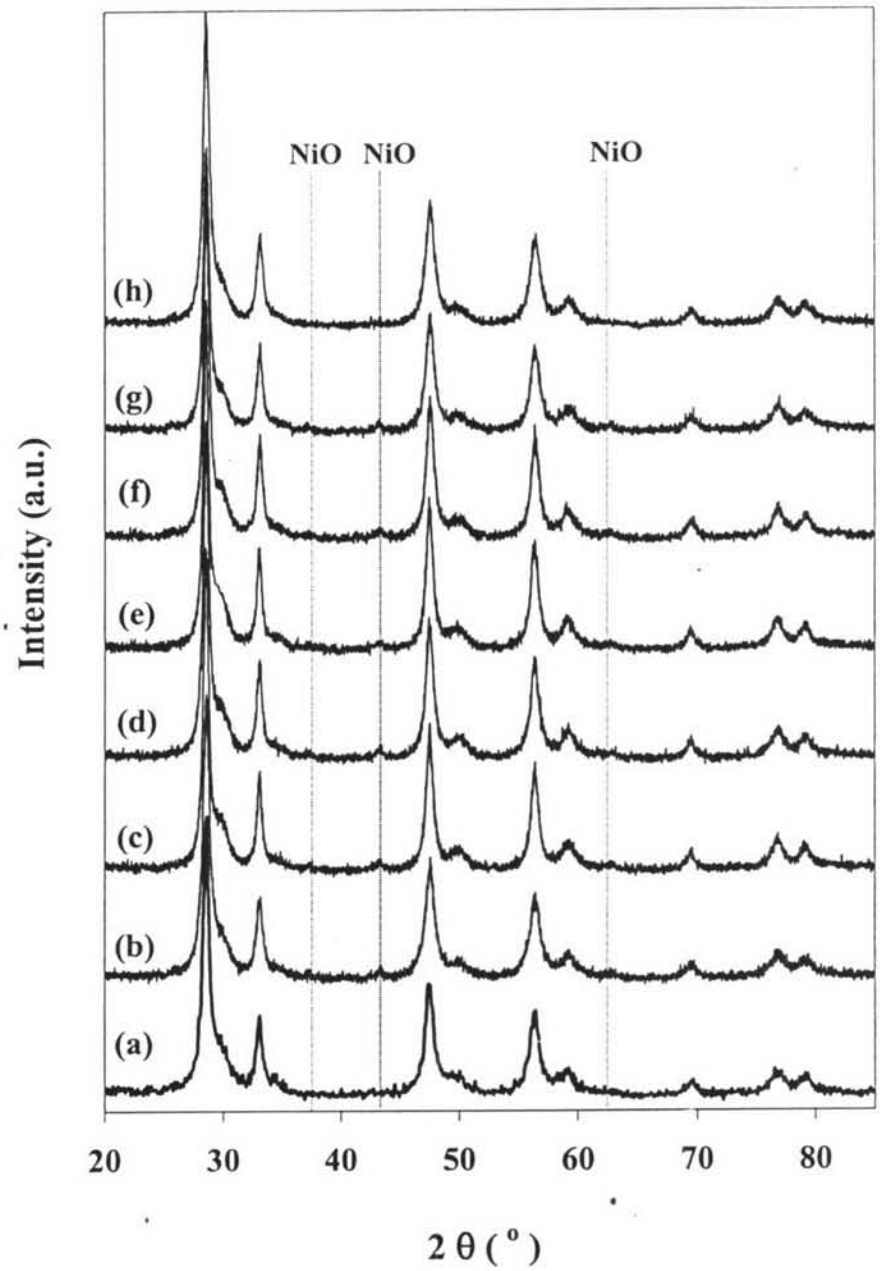

Figure 6.1 XRD patterns for the Ni-Sn over $Ce_{0.75}Zr_{0.25}O_2$ catalysts calcined at 500°C: (a) $Ce_{0.75}Zr_{0.25}O_2$ (b) 5Ni00Sn; (c) 5Ni01Sn; (d) 5Ni03Sn; (e) 5Ni05Sn; (f) 5Ni10Sn; (g) 5Ni20Sn and (h) 2wt%Sn/$Ce_{0.75}Zr_{0.25}O_2$.

6.4.3 H_2-TPR

Figure 6.2 shows the H_2-TPR profiles of Ni-Sn over $Ce_{0.75}Zr_{0.25}O_2$ catalysts calcined at 500°C prepared by co-impregnation. The TPR profile of the pure support shows two reduction peaks at temperatures of about 550 °C and 800 °C. The sample containing 2 wt% Sn exhibits a SnO reduction peak at about 330 °C, but the support reduction peaks are very weak. One possible explanation could be that Sn, once reduced, melts at higher temperature and spreads over the support, thus preventing further reduction of the support.

For the profile of 5 wt% $Ni/Ce_{0.75}Zr_{0.25}O_2$, it can be seen that the reduction peaks of the sample were occurred at temperature ≈ 300, 370°C and other broad peak at temperature over 800°C. The first two peaks indicate the reduction of NiO to Ni^0 and the other is the reduction of support (Montoya *et al.*, 2000). Generally, for supported Ni catalysts the lower temperature peaks are attributed to the reduction of the relatively free NiO particles, while the higher temperature peaks are the reduction of complex NiO species in intimate contact with the oxide support (Roh *et al.*, 2002). The peak at 300°C becomes more pronounced with increasing amount of Sn, and the peak temperature shows a slight shift to higher temperatures which can be rationalized by superposition of the low temperature NiO-reduction peak with the SnO reduction peak occurring at slightly higher temperature. The fact that adding Sn leads to the growth of the low temperature peak indicates that as Sn loading increases, the relative concentration of free NiO particles increases. Based on the TPR results, it appears that SnO species somehow interfere with the support interactions between NiO and the ceria-zirconia. Adding Sn does, however, not affect the reduction temperature of the ceria-zirconia support.

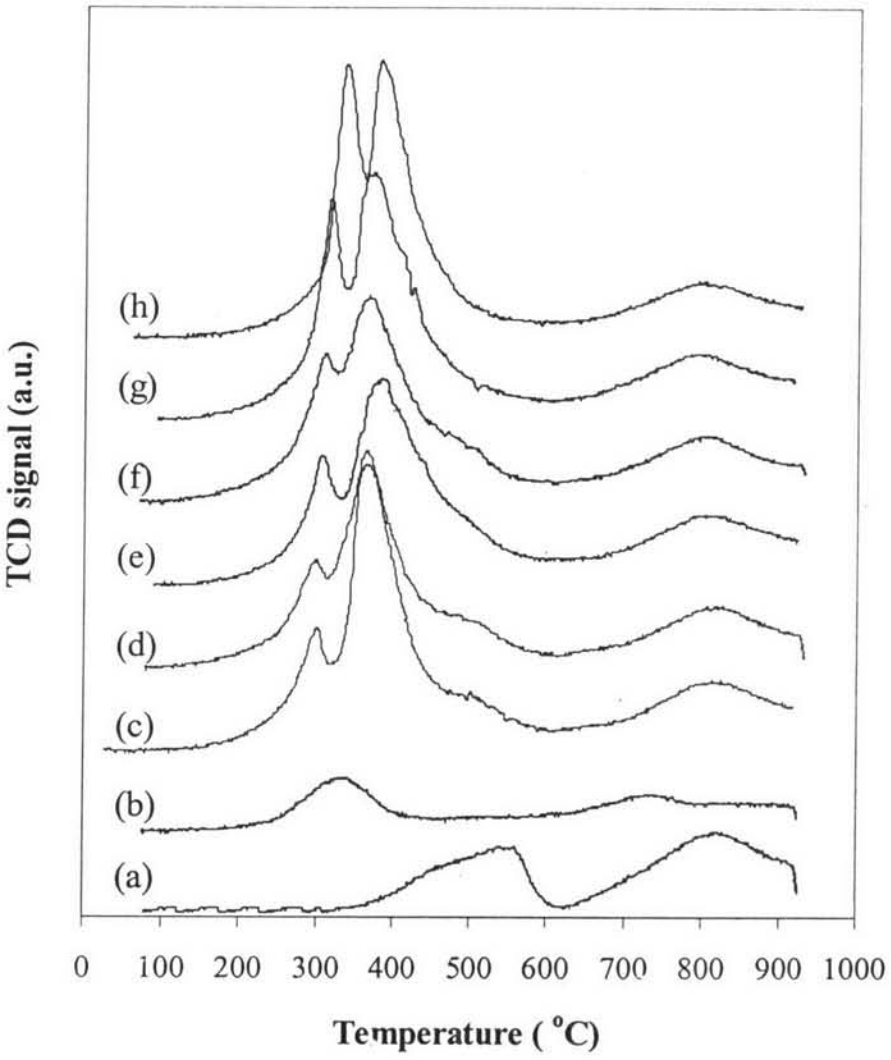

Figure 6.2 H_2-TPR profiles for catalysts calcined at 500°C with a heating rate of 10 °C min^{-1}, a reducing gas containing 5% hydrogen in nitrogen with a flow rate of 30 ml min^{-1}: (a) $Ce_{0.75}Zr_{0.25}O_2$; (b) 2 wt%Sn/$Ce_{0.75}Zr_{0.25}O_2$; (c) 5Ni00Sn; (d) 5Ni01Sn; (e) 5Ni03Sn; (f) 5Ni05Sn; (g) 5Ni10Sn and (h) 5Ni20Sn.

6.4.4 TEM and High Resolution Transmission Electron Microscopy

Figures 6.3 – 6.6 show the typical TEM images of 5Ni00Sn; 5Ni01Sn, 5Ni05Sn and 5Ni10Sn catalysts. From the TEM image of 5Ni00Sn, the particle size of the sample is almost in the range of 15-20 nm. This result is in agreement with the average Ni particle size determined from H_2 chemisorption by assuming the stoichiometry of H_2:Ni = 2:1 about 17.8 nm.

For Ni-Sn samples, like Ni00Sn sample, the particle sizes of the samples are not much changed with increasing amount of Sn loadings. There are mostly in the range of 15-20 nm. This result indicated that the addition of Sn does not change significantly the particle size. However, this result did not agree with the result of average Ni particle sizes determined from the H_2 chemisorption. The particle sizes determined by H_2 chemisorption of 5Ni01Sn, 5Ni05Sn and 5Ni10Sn samples are about 22.0, 45.5 and 72.5 nm, respectively. From the experiment, Sn did not adsorb H_2 under our experimental conditions. Therefore, this result confirmed that presence of Sn interferes with the uptake of H_2 on Ni possibly by blocking Ni surface sites or by preventing the complete reduction of NiO to Ni.

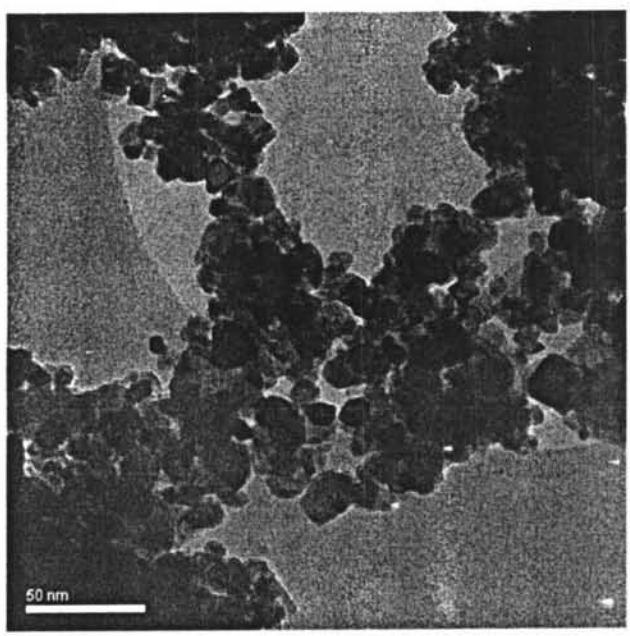

Figure 6.3 TEM image of 5Ni00Sn catalyst.

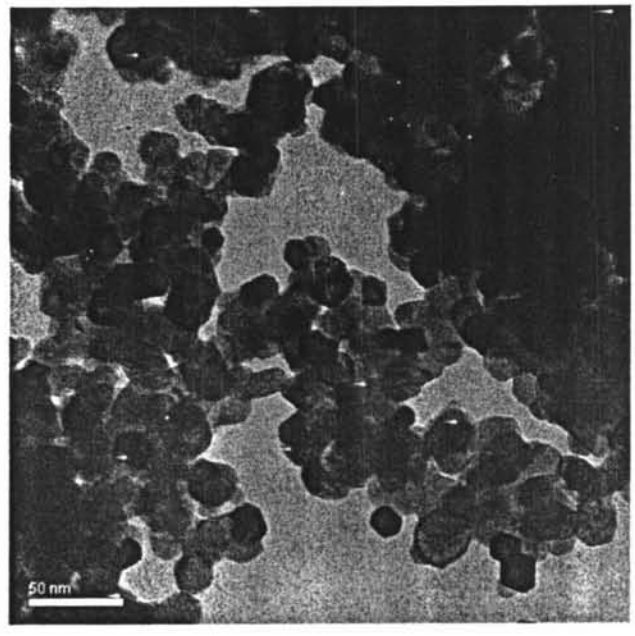

Figure 6.4 TEM image of 5Ni01Sn catalyst.

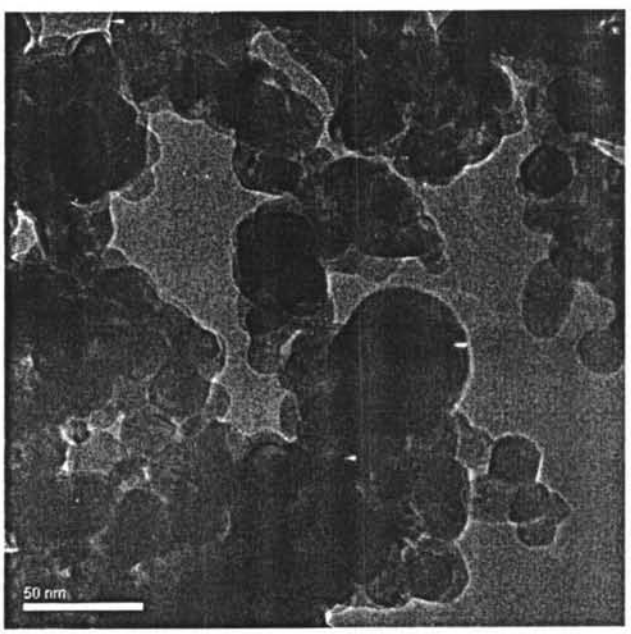

Figure 6.5 TEM image of 5Ni05Sn catalyst.

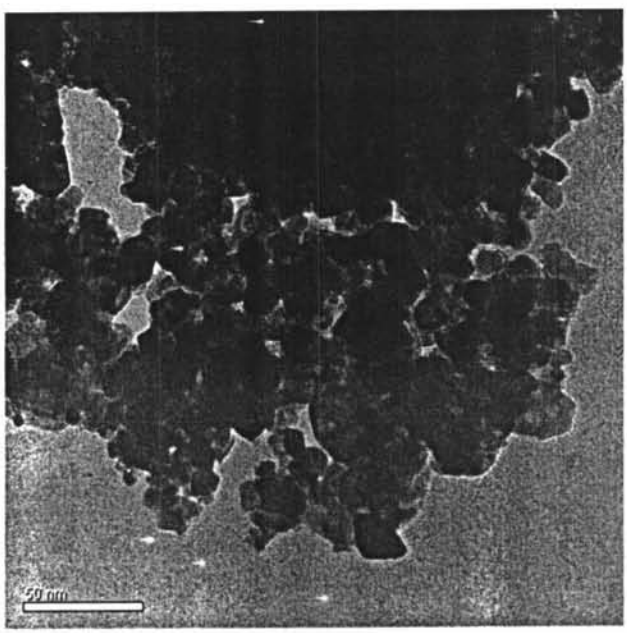

Figure 6.6 TEM image of 5Ni10Sn catalyst.

HRTEM structural images of 5Ni01Sn and 5Ni10Sn samples are shown in Figures 6.7 and 6.8. The HRTEM images of the two samples showed the FCC structure of NiO. The Fourier transform of one of these particles showed a cubic structure with lattice parameters of 0.41 nm. This structure can be assigned to a NiO by comparison with the lattice parameter. No evidence of the formation of Ni-Sn alloys was found by HRTEM. Attempts to detect Sn location by EDX were unsuccessful. It appears that Sn is spread out over the Ni particles and support and/or due to the lower amount of Sn could be detected by EDX. We know that the presence of Sn affects the Ni dispersion. However, this raises the question of where the Sn is located. One possibility is that Sn decorates the surface of these Ni particles and would not be visible in HRTEM images. Therefore, HRTEMs have to be interpreted in conjunction with H_2 chemisorption. From H_2 chemisorption result, the amount of H_2 consumption decreased with increasing amount of Sn loadings. This suggests that Sn which does not adsorb H_2, decorates the Ni particles and blocks some of the active Ni surface sites. This phenomena is in agreement with the HRTEM observation of Sn alloys in Pt-Sn/C, Pt-Sn/SiO_2 (Neri *et al.*, 2002) and Ru-Sn/C catalysts (Neri *et al.*, 1994). They conclude that the majority of the surface of metal particles was decorated by Sn without any evidence for bulk alloy formation.

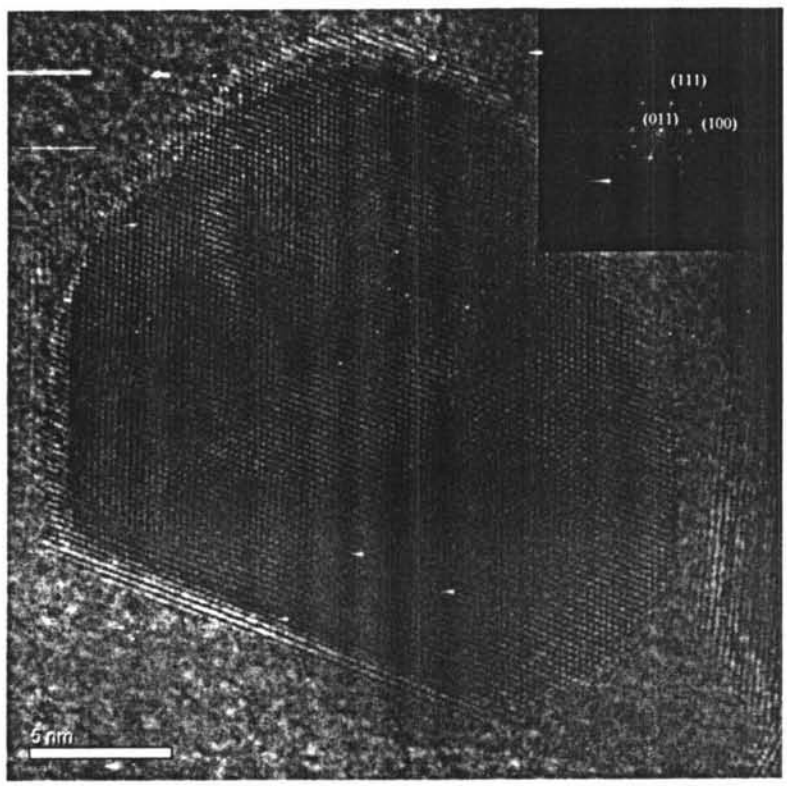

Figure 6.7 HREM image of 5Ni01Sn catalyst.

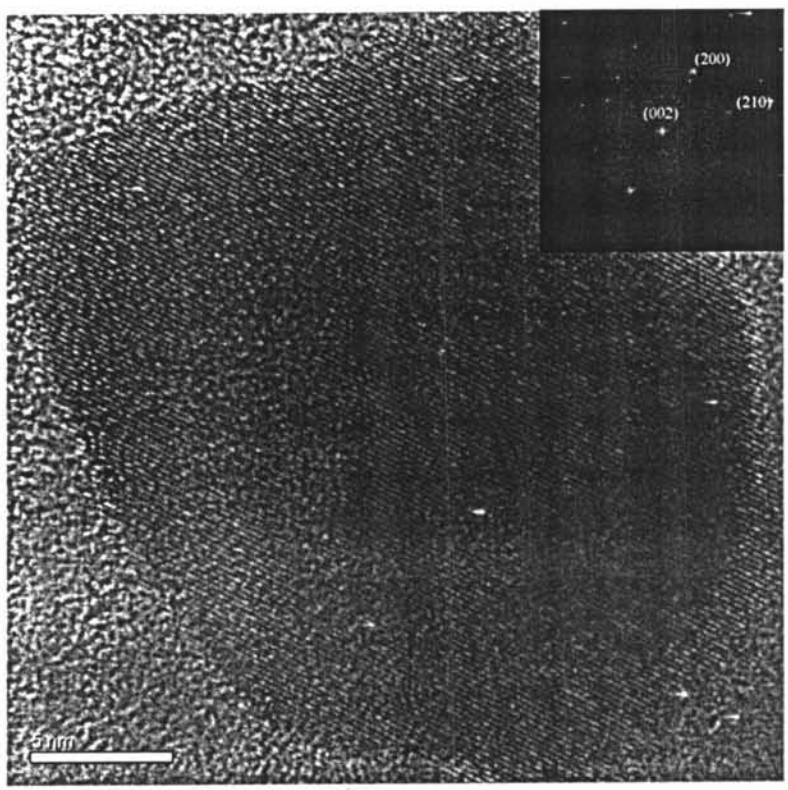

Figure 6.8 HREM image of 5Ni10Sn catalyst.

6.4.5 Catalytic activities for methane partial oxidation

Figure 6.9 and 6.10 show the results of the catalytic activity test of MPO over the Ni-Sn catalysts. For the 5Ni00Sn catalyst, synthesis gas started to form at temperatures above 550°C. Adding Sn caused the light-off temperature to shift to higher temperatures. For low amount of Sn loadings (0.1-0.5 wt%), synthesis gas was started at temperature above 600°C and shifted to higher temperatures with increasing amount of Sn loadings. This might be due to some of Sn particles covering Ni particles. There is a general agreement that the dissociative adsorption of CH_4 to form a carbonaceous intermediate occurs over Ni surfaces. For the Ni-Sn samples, Ni particles covered by Sn would thus require a higher temperature to melt Sn and open up Ni particle.

As shown in Figures 6.9 and 6.10, it is observed that the catalytic activity (both of the methane conversion and the synthesis gas selectivity) was not appreciably affected by small amount of Sn loadings (0.1-0.5 wt%). For higher amount of Sn loadings (> 0.5 wt%), as the Sn loading increases, the methane conversion and synthesis gas selectivities were significantly decreased. This might be due to the fact that the Ni surface is only partially covered with Sn species. Interestingly, the catalytic activity of 5Ni20Sn is very similar to that of the 2 wt% $Sn/Ce_{0.75}Zr_{0.25}O_2$ catalyst. This suggests that at this amount of Sn loading, the NiO particles are fully covered by Sn species. In this case, the surface enriched Sn would hinder the access of CH_4 on the surface of Ni particles and depress its activity.

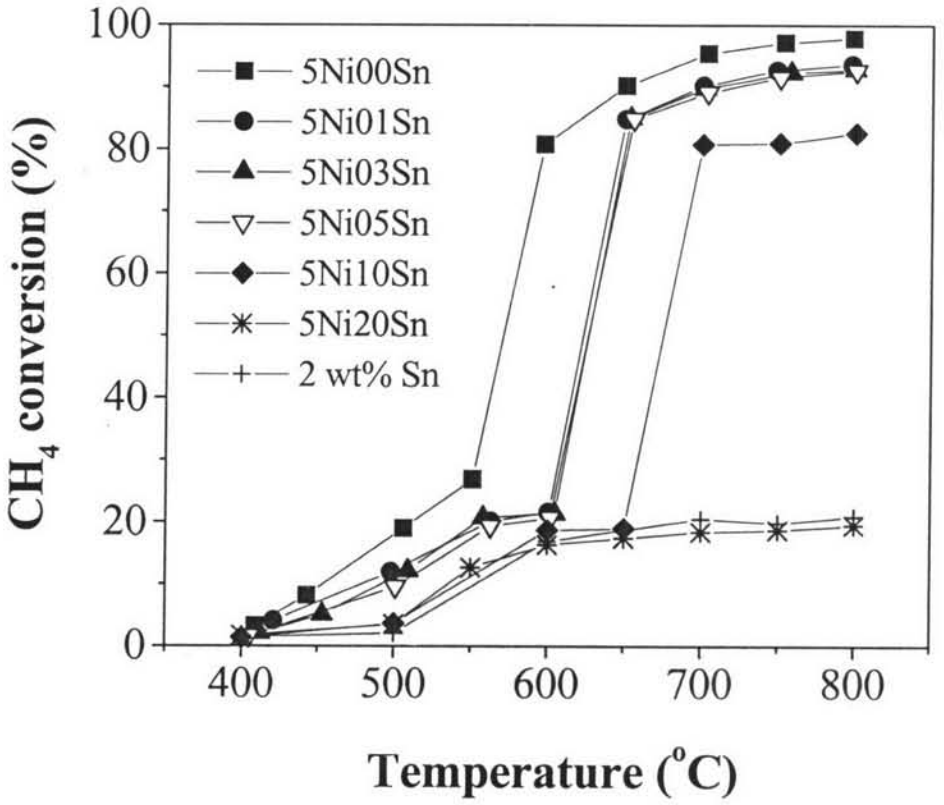

Figure 6.9 Methane conversion at different temperature over Ni-Sn/$Ce_{0.75}Zr_{0.25}O_2$ catalysts (CH_4/O_2 ratio of 2.0, GHSV = 53,000 h^{-1}).

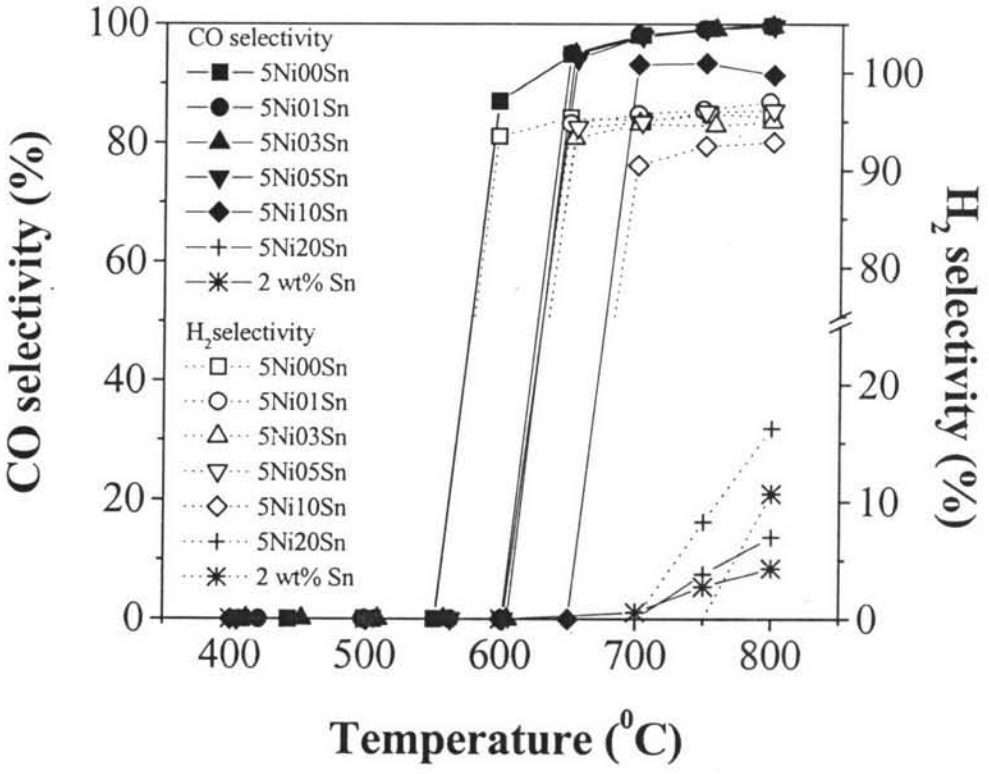

Figure 6.10 CO and H_2 selectivities over Ni-Sn/$Ce_{0.75}Zr_{0.25}O_2$ catalysts (CH_4/O_2 ratio of 2.0, GHSV = 53,000 h^{-1}).

6.4.6 Carbon deposition

The amount of carbon deposition on the catalysts after 24 h of reaction at 750°C and CH_4/O_2 ratio of 2 are shown in Table 6.2. The amount of carbon deposition on the spent catalysts was quantified by TPO technique. As shown in Table 6.2, the amount of carbon deposition was found to decrease sharply by more than 50% with small amounts of Sn loadings. This indicated that the carbon deposition is strongly inhibited in the presence of very low Sn concentrations. The catalytic results presented in the previous section show the important effect of tin loading. For the lower Sn loadings (< 0.5 wt%), the carbon deposition is almost completely inhibited while the catalytic activity for MPO only slightly dropped for these compositions. This led us to the question of what the role of Sn is on inhibition of carbon deposition.

From the characterization results (H_2 chemisorption, XRD, H_2-TPR and TEM) it is reasonable to postulate that Sn does not form Ni-Sn alloys and must be covering the surface of Ni particles. Since coke formation would require a larger ensemble of active Ni sites than methane partial oxidation (Trimm, 1999, Nichio *et al.*, 2000), partial overlayers of Sn species appear very effective tc destroy many of the active sites for coke formation. These results are confirmed by TEM images of spent catalysts as shown in Figures 6.11 and 6.12. It was observed that whisker carbons are formed on spent 5Ni03Sn catalyst while they can not be seen in spent 5Ni10Sn. It can be concluded that the partial coverage of Ni particles by Sn could reduce the growth of whisker carbon. This result is in agreement with the study of Sn doped Ni/Al_2O_3 reported by Padeste *et al.* (1993).

Table 6.2 The amount of carbon deposition quantified by TPO over the catalysts after 24 hr of reaction at 750^0C and CH_4/O_2 ratio of 2.0

Catalyst code	CH_4 Conversion[1] (%)	Amount of carbon deposition (wt%)
5Ni00Sn	97	8.56
5Ni01Sn	93	4.13
5Ni03Sn	90	0.86
5Ni05Sn	81	0.24
5Ni10Sn	28	0.22
5Ni20Sn	15	0.12

[1]at the end of reaction time (24hr)

6.5 Conclusions

It can be concluded that the addition small amounts of Sn (<0.5 wt%) into $Ni/Ce_{0.75}Zr_{0.25}O_2$ catalyst decreases the amount of carbon deposition, while maintaining most of the catalytic activity for MPO. This might be due to partial coverage of NiO particles with Sn species, disrupting the active site ensembles responsible for coking. When added in high amounts, a total coverage of Ni particles by Sn leads to loss of catalytic activity. Furthermore, Sn could also reduce the amount of whisker carbon growth by retarding the solubility of carbon in Ni particles.

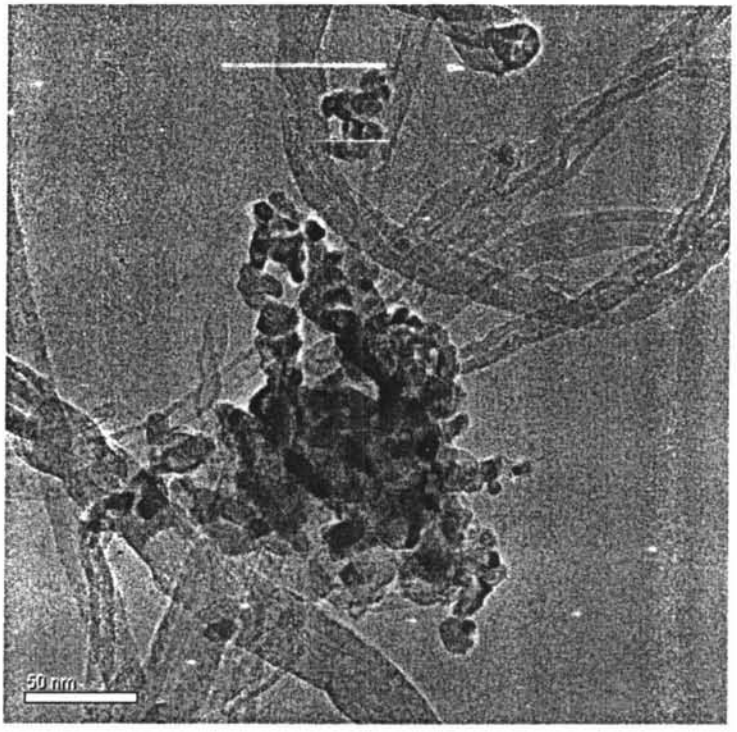

Figure 6.11 TEM image of spent 5Ni03Sn catalyst after exposure to MPO reaction at 750°C (CH_4/O_2 = 2.0, GHSV = 53,000 h^{-1}) for 24 h.

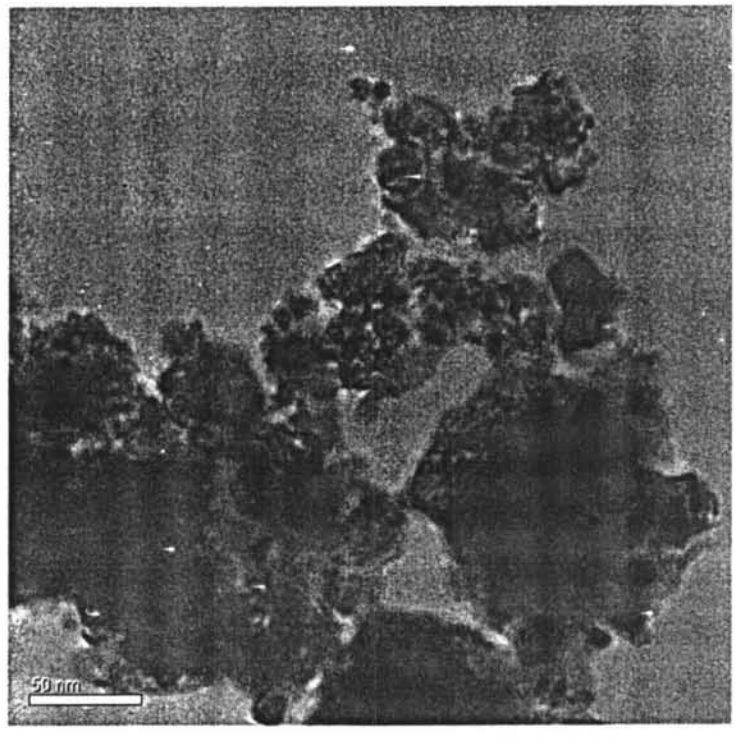

Figure 6.12 TEM image of spent 5Ni10Sn catalyst after exposure to MPO reaction at 750°C (CH_4/O_2 = 2.0, GHSV = 53,000 h^{-1}) for 24 h.

6.6 Acknowledgments

The authors would like to thank RGJ, Ph.D.program, Thailand Research Fund and for the financial support. We thank Dr. Kai Sun of the University of Michigan Electron Microbeam Analysis Laboratory for valuable assistance in the microscopy work.

6.7 References

Boucouvalas, Y., Zhang, Z., Verykios, X. E. (1996) Partial oxidation of methane to synthesis gas via the direct reaction scheme over Ru/TiO2 catalyst. Catalysis Letters, 40, 189.

Dissanayake, D., Rosynek, M. P., Kharas, K.C.C. and Lunsford, J.H. (1991) Partial Oxidation of Methane to Carbon Monoxide and Hydrogen over a Ni/Al_2O_3 Catalyst. Journal of catalysis, 132, 177.

Ferreira M.J., Nichio N.N. and Ferretti O.A. (2003) A semiempirical theoretical study of Ni/α-Al_2O_3 and $NiSn/\alpha$-Al_2O_3 catalysts for CH_4 reforming. Journal of molucular catalysis A: Chemical 202, 197.

Hickman D.A. and Schmidt L.D. (1993) Production of syngas by direct catalytic oxidation of methane. Science, 259, 343.

Hou Z., Yokota O., Tanaka T. and Yashima T. (2004) Surface properties of a coke-free Sn doped nickel catalyst for the CO_2 reforming of methane. Applied Surface Science, 233, 58.

Irigoyen, B. Castellani, N. and Juan.A. (1998) Methane oxidation reaction on MoO_3 (100): A theoretical study. Journal of Molecular Catalysis A: Chemical, 129, 297.

Lu Y., Xue J., Yu C., Liu Y. and Shen S., (1998) Mechanistic investigations on the partial oxidation of methane to synthesis gas over a nickel-on-alumina catalyst. Applied Catalysis A: General, 174, 121.

Montoya, J.A., Romero-Pascual, E., Gimon, C., Del Angle, P., Monzon, A., (2000) Methane Reforming with CO_2 over Ni/ZrO_2-CeO_2 Catalysts Prepared by Sol-Gel. Catalysis Today, 63, 71.

Neri G., Plietropaolo R., Galvagno S., Milone C. and Schwank J. (1994) Characterization of carbon supported ruthenium-tin catalysts by high-resolution electron microscopy. Journal of the chemical society. Faraday transactions, 90, 2803.

Neri G., Milone C., Galvagno S., Pijpers A.P.J. and Schwank J. (2002) Characterization of Pt-Sn/carbon hydrogenation catalysts, Applied Catalysis A: General 227, 105.

Nichio N.N., Casella M.L., Santori G.F., Ponzi E.N. and Ferretti O.A. (2000) Stability promotion of Ni/α-Al_2O_3 catalysts by tin added via surface organometallic chemistry on metals: Application in the methane reforming processes. Catalysis Today, 62, 231.

Onda A., Komatsu T. and Yashima T. (2001) Preparation and catalytic properties of single-phase Ni-Sn intermetallic compound particles by CVD of $Sn(CH_3)_4$ onto Ni/Sillica. Journal of Catalysis, 201, 13.

Otsuka K., Wang Y., Sunada E. and Yamanaka I. (1998) Direct partial oxidation of methane to synthesis gas by cerium oxide. Journal of Catalysis, 175, 152.

Otsuka K., Wang Y. and Nakamura M., (1999) Direct conversion of methane to synthesis gas through gas-solid reaction using CeO_2-ZrO_2 solid solution at moderate temperature. Applied Catalysis A: General, 183, 317.

Pantu P., Kim K. and Gavalas G.R. (2000) Methane partial oxidation on Pt/CeO_2-ZrO_2 in the absence of gaseous oxygen. Applied Catalysis A: General, 193, 203.

Pedeste C., Trimm D.L. and Lamb R.N. (1993) Characterization of Sn doped Ni/Al_2O_3 steam reforming catalysts by XPS. Catalysis Letters, 17, 333 .

Pengpanich S., Meeyoo V., Rirksomboon T. and Bunyakiat K. (2002) Catalytic oxidation of methane over CeO_2-ZrO_2 mixed oxide solid solution catalysts prepared via urea hydrolysis. Applied Catalysis A: General, 234, 221.

Pengpanich S., Meeyoo V. and Rirksomboon T. (2004) Methane partial oxidation over Ni/CeO_2-ZrO_2 mixed oxide solid solution catalysts. Catalysis Today, 93-95, 95.

Roh. H., Jun, K., Dong, W., Chang, J., Park, S., and Joe, Y. (2002) Highly Active and Stable Ni/Ce-ZrO_2 Catalyst for H_2 Production from Methane. Journal of Molecular Catalysis A: Chemical, 181, 137

Rostrup-Nielsen J.R. and Alstrup I. (1999) Innovation and science in the process industry steam reforming and hydrogenolysis. Catalysis Today, 53, 311.

Ruckenstein E. and Hu H.Y. (1999) Methane partial oxidation over NiO/MgO solid solution catalysts. Applied Catalysis A: General, 183, 85.

Trimm D.L. (1999) Catalysts for the control of coking during steam reforming. Catalysis Today 49, 3.

Zhu, T., and Flytzani-Stephanopoulos, M. (2001) Catalytic Partial Oxidation of Methane to Synthesis gas over Ni-CeO_2. Applied Catalysis A: General, 208, 403.